WOOD RESEARCH doi.org/10.37763/wr.1336-4561/71.1.166177
e-ISSN 2729-8906
71(1): 2026 166-177 pp.

DYNAMIC DETECTION THE DAMAGE AND FRACTURE PROCESS OF LOAD-BEARING WOOD USING ACOUSTIC EMISSION TECHNOLOGY

KUN DU[1], LIJIAN YUAN[2], YOULI WANG[2], XINLIN LI[1], MING LI[3,4], SAIYING FANG[1], HAO SHI[1], YONGYOU CHEN[1], XUANRUI GONG[1]
[1]SOUTHWEST FORESTRY UNIVERSITY, CHINA
[2]YUNNAN VOCATIONAL INSTITUTE OF ENERGY TECHNOLOGY, CHINA
[3]ANHUI POLYTECHNIC UNIVERSITY, CHINA
[4]KEY LABORATORY OF ADVANCED PERCEPTION AND INTELLIGENT CONTROL OF HIGH-END EQUIPMENT OF MINISTRY OF EDUCATION, CHINA

RECEIVED JANUARY 2026

ABSTRACT

This research utilizes three-point bending experiment to simulate actual load-bearing scenarios of wood, and uses acoustic emission monitoring system to collect real-time acoustic emission signal parameters, such as ringing count, energy, amplitude, etc. Analyze the relationship between acoustic emission signals and internal damage during different loading stages, and construct an acoustic emission recognition model for damage and fracture process of elm. Research result shown that during elastic deformation and early plastic deformation stage, the activity of acoustic emission is weak, mainly due to damage and delamination at cell wall, and cell wall buckling and collapse. Entering plastic deformation stage, acoustic emission ringing count and energy significantly increase, corresponding to a large number of cell wall ruptures and microcrack initiation. Near macroscopic fracture stage, high-intensity and high-energy acoustic emission signal clusters appear, indicating rapid propagation of main crack and ultimately leading to fracture.

INTRODUCTION

Acoustic emission (AE) is a phenomenon in which material or structure undergoes microscopic or macroscopic damage due to external loads or internal state changes, resulting in instantaneous release of strain energy and the generation of elastic stress waves (Liu et al. 2002, Vun et al. 2005, Baensch,Sause, et al. 2015, Baensch,Zauner, et al. 2015, Diakhate et al. 2017, Du et al. 2025). By capturing AE signals through high-sensitivity sensor, then amplifying, processing, and analyzing the signals, information such as location, type, and development trend of internal damage can be inferred (Fang et al. 2023, Du,Wang, et al. 2024). From

the perspective of non-destructive testing, AE technology can help solve problems such as when damage occurs inside components or materials, what kind of damage it is, where damage occurs, and how severe the damage is (Jeng et al. 1988, Shen et al. 2015, Li et al. 2020, Ding et al. 2021, Li, Y. et al. 2021, Liu 2021, Qin et al. 2024). Researching the development process of wood damage and fracture under load conditions based on AE signal parameters can reveal corresponding relationship between formation and propagation of wood cracks and AE activity characteristics (Noguchi et al. 1985, Kowalski et al. 2004, Mohammadi et al. 2015, Rescalvo et al. 2020). AE technology is particularly important for wood structures that gradually accumulate damage during long-term use, as it can provide early warning of potential safety hazards. By deploying multiple AE sensors on wood and utilizing multi-channel data acquisition and analysis system, comprehensive monitoring of wood damage and fracture can be achieved (Wang,Li, et al. 2021, ZHAI et al. 2025). In addition, even in cases of mild damage, researching the damage situation through characteristic parameters of AE signals can help take measures in early stages of damage.

This research aims to use AE technology to monitor and analyze damage and fracture process of load-bearing elm specimen in real-time and accurately. By collecting and researching AE signals, dynamic monitoring of factors such as the time, trend, and severity of internal cracks is carried out. Master the activity of dynamic cracks and defects inside wood, and find the "critical point" where wood is about to break. By exploring mechanism of AE signals, the relationship between AE signal characteristic parameters and wood damage and fracture is studied.

MATERIALS AND METHODS

Air-dried elm specimen is sawn into dimensions of 300 mm (axial) × 20 mm (tangential) × 20 mm (radial). In this research single resonant AE sensor (Beijing Soundwel Technology Co., Ltd., Beijing, China) is fixed 80 mm from left end face of specimen with rubber tape, the schematic diagram and physical image of experimental setup are shown in Fig. 1. This research utilizes universal mechanical testing machine to load in middle of specimen, and the pressure head of testing machine is advances in a speed of 2 mm/min, the load is applied parallel to annual rings. Vacuum-insulating grease is applied between specimen and AE sensor to assure effective coupling.

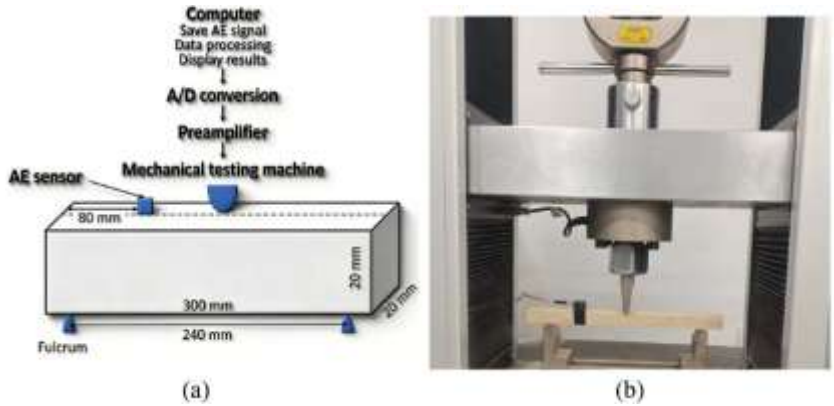

Fig. 1: Schematic diagram (a) and physical image (b) of experimental setup.

The density and moisture content of elm specimen are 680±5 kg/m^3 and 10.4±0.5%. The determination method of wood density and moisture content is according to GB/T 1933-2009 and GB/T 1931-2009. A three-channel high-speed data acquisition system is being built using NIUSB-6366 acquisition card (National Instruments, USA) and LabVIEW (National Instruments, USA). The system will extract AE signals generated during wood damage and fracture process. The frequency response range of this AE sensor is 10~220 kHz. The gain of PAI preamplifier (Beijing Soundwel Technology Co., Ltd., Beijing, China) is 40 dB, and the output voltage range of amplifier is set to −5 to 5 V. The amplifier is equipped with a device for amplifying AE signals and reducing noise. Related studies have shown that the peak frequency of AE signals generated during wood damage and fracture process is within 200 kHz (Li et al. 2020, Li, M. et al. 2021, Wang,Li, et al. 2021, Ding et al. 2022, Qin et al. 2022, Du,Li, et al. 2024, ZHAI et al. 2025). In order to recover AE signals without distortion, sampling frequency should be at least twice maximum frequency. Therefore, in this research the sampling frequency is set to 500 kHz.

RESULTS AND DISCUSSION

Fig. 2a illustrates the time-load curve during the damage and fracture process of elm specimen. From 0 to about 30 seconds, the load shows linear growth trend, indicating that elm specimen is in elastic deformation stage. Cell wall structure of wood (fibers, tracheids, etc.) undergoes reversible deformation under stress, supported by the bending of cell wall and elastic stretching of tracheids (Shao 2007, 2009, Diakhate et al. 2017, Du et al. 2025). At this stage, slope of the time-load curve remains almost unchanged, reflecting the stability of apparent elastic modulus of specimen, which conforms to Hooke's law. The load gradually exceeds 500 N, indicating that specimen has high stiffness along grain direction, but due to the anisotropic characteristics of wood, lateral strain may have begun to accumulate micro damage. Roughly from 30 to 90 seconds, the rate of load growth gradually decreases, and the curve exhibits nonlinear characteristics, indicating that specimen has entered transitional stage of elastic-plastic deformation. Cell wall of wood begins to undergo irreversible deformation: fibers in some weak areas slip or bend locally (Zhang et al. 2021, Fang et al. 2022, Fang et al. 2023).

Fig. 2b shows the flexural stress-deformation curve, which fully demonstrates the deformation at middle position of specimen during the process of increasing flexural stress from 0 to maximum. According to GB/T 1927.9-2021, the calculation formula for flexural stress of wood is as follows:

$$\sigma = \frac{3Pl}{2bh^2} \tag{1}$$

where: P represents load, with the unit being N, l, b, and h represent span between two supports, the width and height of specimen, respectively, with all units being mm.

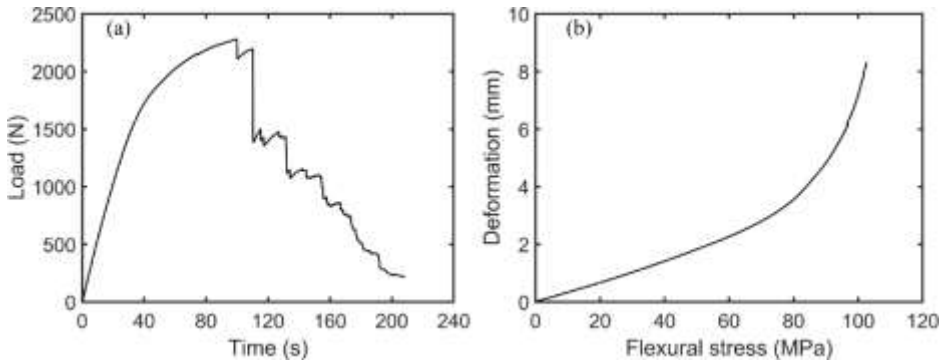

Fig. 2: (a) Time-load curve and (b) The deformation at the middle position of the specimen during the process of increasing the flexural stress from 0 to the maximum value.

After 80 seconds, the load gradually approaches its peak value (about 2200 N), at which point the overall strength of specimen reaches dynamic equilibrium with stress concentration effect. Roughly from 90 to 110 seconds, the sudden drop and fluctuation after peak load reveal intense energy release. When maximum tensile stress exceeds the tensile strength of specimen, macroscopic cracks first appear on tensile side, and the bearing capacity significantly decreases. The fluctuation characteristics of time-load curve correspond to dynamic propagation behavior of cracks: high stress at crack tip causes local fibers to gradually fracture, and each fracture event triggers a sudden drop in load, while bridging effect of unbroken fibers promotes a brief rebound in load (Wang,Li, et al. 2021, Qin et al. 2022). From approximately 110 to 200 seconds, the load enters a stepped decay channel, indicating that specimen has entered a stable fracture stage. While main crack continues to propagate, secondary cracks initiate under shear stress, forming fracture process zone. The layered structure of wood causes cracks to break through bonding interface between fiber bundles in stages, and each interface debonding corresponds to load plateau period. The residual load is maintained by friction of incompletely separated fibers, contact friction of crack surfaces, and local non failure areas, exhibiting typical ductile fracture characteristics (Kazemi Najafi et al. 2017, Zhang et al. 2021). Approximately 200 seconds later, load gradually approaches zero, indicating that specimen is gradually losing its load-bearing capacity. There is only weak contact load between completely separated fracture surfaces, which may be due to dynamic contact caused by interlocking between fragments or environmental vibrations.

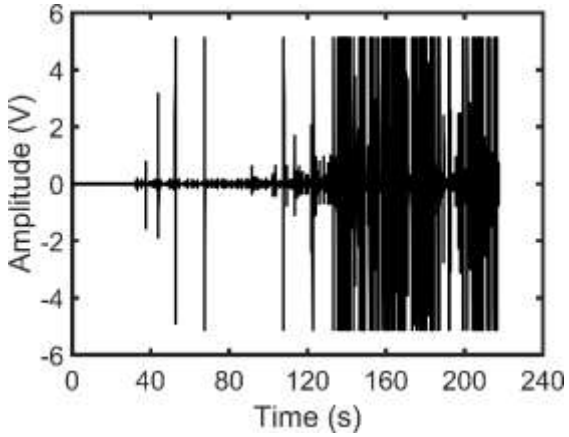

Fig. 3: Time-domain waveform of AE signals during damage and fracture process of elm

specimen.

The time-domain waveform of AE signals during the damage and fracture process is shown in Fig. 3, revealing the dynamic characteristics of internal damage evolution in specimen. Based on time-load curve, the evolution process of AE signals can be divided into several stages. At the beginning of loading, amplitude of AE signals is close to zero baseline, with only weak environmental noise or instrument background fluctuations. Cell wall structure of wood undergoes reversible deformation under stress. As load increases, microcrack zone may gradually generated in end of initial microcrack (Shao et al. 2009). When threshold is exceeded, in addition to microscopic damage, microcrack damage zone will continue to expand (Du,Wang, et al. 2024). As load gradually approaches its peak, fibers in some weak areas experience slippage or local buckling. Each AE signal corresponds to a damage or fracture event: when microcracks form or fiber bundles break, stored elastic strain energy is instantly released, generating detectable AE signal. At this stage the damage or fracture AE events of specimen show isolated distribution, reflecting that specimen releases stress through local failure, but continuous cracks have not yet formed. After load reaches its peak, AE signals exhibit continuous fluctuations of high density and amplitude, forming a "signal storm". High amplitude AE signal reflects strong elastic waves released by macroscopic fracture events, and the density of AE signal indicates that cracks penetrate cross-section of specimen at a higher speed. This process is accompanied by significant energy dissipation, and AE activity reaches peak intensity of the entire damage and fracture process. With increase of load, in addition to microscopic damages, cell wall rupture or macroscopic fracture of wood fibers may also occur. At around 160 to 200 seconds, AE signals still maintain a high level of activity, but the amplitude distribution exhibits fluctuating attenuation characteristics. At this stage main crack has penetrated most of cross-section, and fracture process has shifted to a stable propagation mode: crack advances layer by layer at annual ring interface or between fiber bundles, and each interface debonding or fiber bridging fracture produces medium or high amplitude AE signal. The residual load is maintained by friction of incompletely separated fibers, the contact friction of crack surfaces, and local non failure areas, exhibiting typical ductile fracture characteristics. The attenuation trend of AE signal reflects the gradual reduction of remaining bearing section, and energy released by a single fracture event gradually decreases. After about 200 seconds, AE activity gradually decreases, and amplitude of AE signal gradually returns to baseline level, leaving only trace amount of contact noise. The specimen gradually loses its structural integrity, possibly due to interlocking effect between fragments or dynamic contact caused by environmental vibrations, resulting in decreasing amplitude of AE signals. The density of high amplitude AE signals and load peak have spatiotemporal synchronization, verifying real-time monitoring ability of AE technology for structural failure. By researching distribution characteristics of AE signals, the strain energy release characteristics of wood damage and fracture can be quantitatively characterized, providing key data support for evaluating health status of wood structures.

Extract all AE signals generated by elm specimen during damage and fracture process. Based on signal correlation principle, 5 layers wavelet decomposed detail signals are adaptively reconstructed (Du,Wang, et al. 2024). Figs. 4a and 4b show time-domain waveform and spectrum of an AE signal during damage and fracture process. The peak frequency of this signal

is 2.89 kHz, which is lower than frequency response bandwidth of AE sensor used in research. This is mainly because AE signals with low energy and short duration, noise accounts for a large proportion (Wang,Deng, et al. 2021, Xu et al. 2023, Du,Li, et al. 2024). Figs. 4c and 4d show time-domain waveform and spectrum of reconstructed signal corresponding to the original signal shown in Fig. 4a and 4b. The low-frequency AE signals may be generated by damage, delamination, bucking or collapse of cell wall layer (Baensch,Sause, et al. 2015, Fang et al. 2022, Du,Wang, et al. 2024).

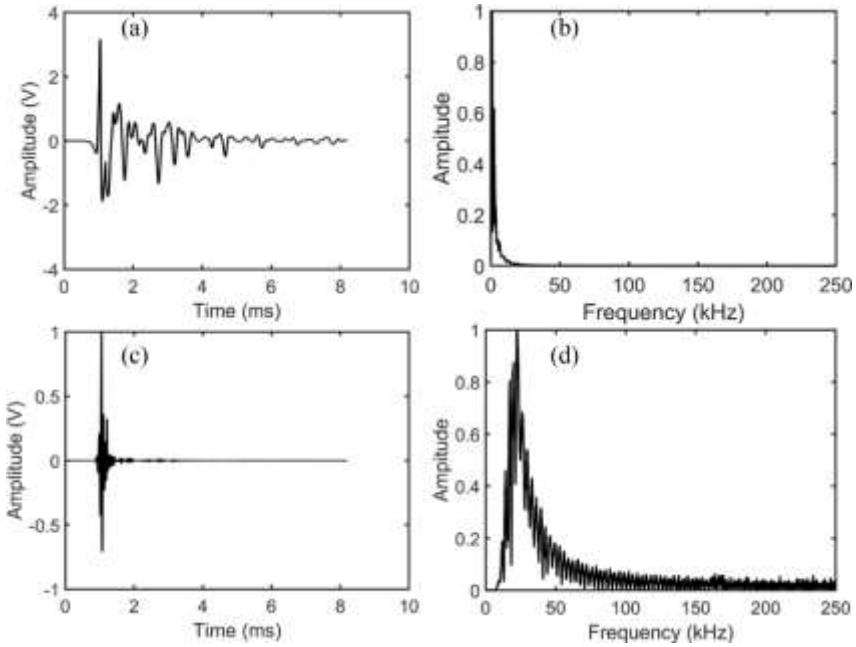

Fig. 4: (a) Time-domain waveform and (b) spectrum of an original signal generated during damage and fracture process. (c)Time-domain waveform and (d) spectrum of reconstructed signal obtained after adaptive wavelet decomposition.

Parameter analysis can be used to conduct in-depth research on AE signals, or to identify the type, intensity, and attenuation characteristics. Amplitude is related to factors such as energy released by AE source and distance between AE source and AE sensor, and it is not affected by threshold voltage and directly determines the measurability of AE event. Fig. 5a shows amplitude distribution of AE signal, demonstrating the temporal variation characteristics. In initial stage, the amplitude is relatively low, scattered in range of 30-50 dB, and data point distribution is relatively sparse. After about 120 seconds, the amplitude significantly increased, and data points were densely distributed in higher amplitude region, indicating increased signal activity and strength. Gradually entering later stage, high amplitude signals gradually decrease, the distribution of AE signals tends to be sparse, and the amplitude falls back to a lower level.

Fig. 5b shows cumulative quantity of AE signals over time. At beginning of this experiment, cumulative number of AE events increased very slowly, and the curve was flat, indicating that there were few and scattered AE events. Entering mid-term stage, the curve sharply rises and cumulative quantity increases rapidly, indicating a significant increase in frequency of AE events and a large accumulation of quantity in a short period of time. In later stage of this experiment, slope of this curve decreased again, the growth trend slowed down and gradually stabilized, and the final cumulative number approached 3800 times, indicating

that incidence of AE events had fallen back to a lower level.

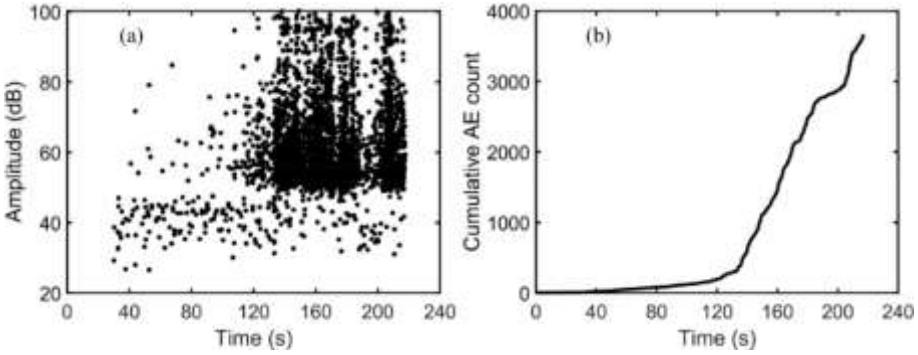

Fig. 5: (a) Amplitude distribution of AE signals and (b) the variation of cumulative number of AE signals.

Energy of AE events is closely related to the degree of deformation and damage occurring inside material. By researching energy changes of AE signals, development of damage inside wood can be monitored. Fig. 6a shows scatter plot of energy distribution of AE signals, with each black dot representing energy value and occurrence time of AE events. Within interval of 0 to 120 seconds, the vast majority of AE events are concentrated in low-energy region, and high-energy AE events are extremely rare during this stage. As time progresses to 120 seconds, the energy distribution s of AE events shows significant changes. The AE event began to spread towards high-energy regions, and within 120 to 200 second interval, the energy distribution range significantly expanded, forming a wide spread pattern. Especially around 160 seconds, there were multiple significant high-energy AE events, with highest energy approaching 5×10^4 μJ。In later stage, the number of high-energy AE events relatively decreases, but there are still some AE events that remain at high energy level. Overall, the temporal distribution of AE events exhibits non-uniformity: in early stages they are characterized by low energy and sparsity, while in middle stages they show increase in energy values and diffusion of distribution. In later stages, they show relative decrease in high-energy events. The range of energy values spans several orders of magnitude, reflecting significant differences in intensity of AE signals.

Fig. 6b shows the trend of accumulated AE signal energy during the damage and fracture process. The curve shows obvious stage characteristics. In initial stage the cumulative energy growth is extremely slow, with this curve almost coinciding with time axis. The data change during this stage is minimal, indicating that AE activity is in relatively silent state. A significant turning point appears at around 120 seconds, and the curve enters an upward channel. During 120 to 200 seconds, the accumulated energy shows an approximately linear acceleration growth, with continuous increase in slope, forming a steep upward segment. At this stage energy accumulation rate reaches its maximum value and jumps from near zero to about 5.4×10^5 μJ within 80 seconds，reflecting that AE events occurred intensively during this period and the energy of AE event significantly increased. After about 200 seconds the slope of this curve gradually decreases and enters a phase of slowing growth rate. Although the accumulation process is still ongoing, the energy increment per unit time begins to decrease, and the curve shows a flattening trend. The curve shape clearly divides the three-stage evolution mode of steady, sudden increase, and gradual decrease, which intuitively reflects the cumulative characteristics of AE energy in damage and fracture process.

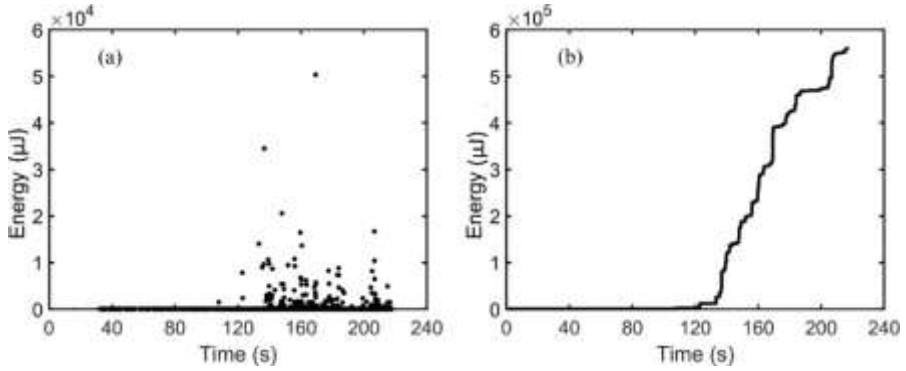

Fig. 6: (a) Distribution diagram of energy of AE signals and (b) variation of accumulated energy of AE signals.

Fig. 6 reveals AE events energy evolution dynamic characteristics during damage and fracture process, providing empirical evidence at microscale for understanding fracture mechanical behavior of wood. This evolutionary model has significant engineering application value. By monitoring temporal characteristics of AE energy during damage and fracture process, a damage state identification index can be established: low-energy AE event reflects the degree of microscopic damage accumulation, and a sudden increase in high-energy events indicates the critical point of structural instability. In addition, the research of the correlation between energy distribution characteristics and wood anatomical structure (such as growth ring density and fiber inclination angle) can provide theoretical support for wood modification and structural optimization. This spatiotemporal resolution of energy evolution research essentially constructs a bridge from microscopic damage to macroscopic fracture, opening up a new dimension for evaluation the mechanical properties of wood.

When using AE technology to dynamically monitor damage and fracture process of wood, the characteristics of AE signals can be clearly captured, and its amplitude does not show a continuous and stable trend, but constantly transitions. This transitional change is like a staircase, where the signal amplitude suddenly jumps from one value to another in short period of time, reflecting discontinuous fluctuation characteristics. From the perspective of entire damage and fracture process, only minor damage occurs inside specimen in early stages, at which point the amplitude and energy of AE signals are relatively low. As damage gradually accumulates, when wood approaches critical state of fracture, internal stress is rapidly released, amplitude and energy of AE signal will significantly increase. Especially at the point of fracture, amplitude and energy of AE signal will reach local maximum, which provides an important basis for accurately determining the location of fracture.

The changes in time and load result in different trends in cumulative quantity and energy of AE signal. In initial stage of loading, which is fully elastic stage, the deformation can be fully restored. With slow increase of time and load, cumulative quantity and energy of AE signal grow relatively slowly. This is because there is only slight elastic deformation inside wood, with almost no irreversible damage, and AE activity is not active. As load further increases, the wood enters a stage of coexistence of elasticity and plasticity dominated by elasticity. At this point wood undergoes both elastic deformation and a small amount of plastic deformation.

The increase in cumulative quantity and energy of AE signals has significantly accelerated, indicating initiation of microcracks and other damage activities inside specimen. When load continues to increase, wood enters a stage of coexistence of plasticity and elastic-plastic behavior, where plastic deformation dominates. The cumulative quantity and energy of AE signals will sharply increase, indicating that internal damage is rapidly expanding, with a large number of microcracks interconnected. AE activity becomes extremely frequent and intense, intuitively reflecting significant changes in internal state of the wood.

CONCLUSIONS

The research has shown that AE parameters can reflect mechanical properties and the damage and fracture status. The following conclusions can be drawn: *(1)* Amplitude and energy of AE signals increase from low to high with accumulation of damage, and reach local maximum at fracture time. *(2)* During elastic deformation and early plastic deformation stage, AE event activity is weak. Entering plastic deformation stage, AE ringing count and energy significantly increase. Near macroscopic fracture stage, high-intensity and high-energy AE clusters appears. *(3)* When small cracks appear, gradual increase in AE rate and amplitude changes indicate that it has reached the first "critical point", and fibers have begun to fracture, entering a dangerous phase. As load continues to increase, amplitude and energy rise significantly, and the damage accumulates, reached second "critical point" and entering extremely dangerous stage. The loads at first and second critical points for elm specimen are approximately 50% and 90% of maximum load, respectively.

There are still some shortcomings in this research. The research did not consider impact of wood diversity on AE signal parameters, which limited the generalizability of these experimental results. Repeating this experiment with different wood species may not yield identical data, but similar conclusions may be drawn. It should be emphasized that above shortcomings or deficiencies are based on general research evaluation criteria and relevant knowledge. Although this research has high practical value in non-destructive testing of wood, its shortcomings or deficiencies still need to be fully considered.

ACKNOWLEDGEMENTS

The authors express their sincere appreciation for backing of the Yunnan Provincial Agricultural Joint Special Program (202501BD070001-030, 202401BD070001-121), the Teaching Science Research Project (YB202413), National Natural Science Foundation of China (32160345, 31760182), Startup fund for introducing talents and scientific research of Anhui University of Engineering (2021YQQ037).

REFERENCES

1. Baensch, F., M. G. Sause, A. J. Brunner, et al. (2015). Damage evolution in wood–pattern recognition based on acoustic emission (AE) frequency spectra. *Holzforschung*, *69*(3), 357-365.

2. Baensch, F., M. Zauner, S. J. Sanabria, et al. (2015). Damage evolution in wood: synchrotron radiation micro-computed tomography (SRμCT) as a complementary tool for interpreting acoustic emission (AE) behavior. *Holzforschung*, *69*(8), 1015-1025.
3. Diakhate, M., N. Angellier, R. M. Pitti, et al. (2017). On the crack tip propagation monitoring within wood material: Cluster analysis of acoustic emission data compared with numerical modelling. *Construction and Building Materials*, *156*, 911-920.
4. Ding, R., S. Fang, R. Luo, et al. (2022). Propagation characteristics and energy attenuation law of surface shear waves and internal longitudinal waves in mongolian scotch pine sawn timber based on acoustic emission. *Chinese Journal of Wood Science and Technology*, *36*(01), 36-42.
5. Ding, R., R. Luo, F. Lai, et al. (2021). Straight line location algorithm of wood acoustic emission source based on singular spectrum analysis and signal correlation analysis methods. *Journal of Northwest Forestry University*, *36*(5), 173-178+245.
6. Du, K., M. Li, S. Fang, et al. (2024). Determine the location of acoustic emission source on wood surface by using a wavelet-energy attenuation method. *Wood Material Science & Engineering*.
7. Du, K., Y. Wang, Z. Zhang, et al. (2025). The attenuation characteristics of different frequency components of acoustic emission signal during propagation in elm and pine wood. *Wood Research*, *69*(4), 647-660.
8. Du, K., Y. Wang, Z. Zhang, et al. (2024). Research on frequency-domain characteristics of acoustic emission signals generated during wood damage and fracture process. *Wood Material Science & Engineering*, 1-11.
9. Fang, S., M. Li, T. Deng, et al. (2022). Study on the time-frequency characteristics and propagation law of acoustic emission longitudinal waves in wood grain direction. *Wood Research*.
10. Fang, S., M. Li, W. Li, et al. (2023). Experimental analysis of acoustic emission propagation velocities and energy attenuation law of p and s waves in wood using improved tdoa measurements. *Wood Research*, *68*(1), 112-128.
11. Jeng, J. S., K. Ono, and J. M. Yang. (1988). *Fracture mechanism studies of carbon fiber reinloadd thermoplastic composites by acoustic emission.* Progress in Acoustic Emission. IV, Kobe, Japan.
12. Kazemi Najafi, S., H. Sharifnia, M. Ahmadi Najafabadi, et al. (2017). Acoustic emission characterization of failure mechanisms in oriented strand board using wavelet-based and unsupervised clustering methods. *Wood Science & Technology*, *51*(6), 1433-1446.
13. Kowalski, S. J., W. Molinski , and G. Musielak. (2004). The identification of fracture in dried wood based on theoretical modelling and acoustic emission. *Wood Science & Technology*, *38*(1), 35-52.
14. Li, M., M. Wang, R. Ding, et al. (2021). Study of acoustic emission propagation characteristics and energy attenuation of surface transverse wave and internal longitudinal wave of wood. *Wood Science & Technology*, *55*(6), 1619-1637.
15. Li, X., T. Deng, M. Wang, et al. (2020). Linear positioning algorithm improvement of wood acoustic emission source based on wavelet and signal correlation analysis methods. *Journal of Forestry Engineering*, *5*(3), 138-143.

16. Li, Y., W. Xi, Z. Zhang, et al. (2021). Research status and prospect of rock creep acoustic emission characteristics. *Geology of Gansu*, *30*(2), 66-69.
17. Liu, H., H. Zhang, and Y. Yan. (2002). Application and study progress of acoustic emission technology in composite material. *Fiber Composites*, *2*(04), 50-52.
18. Liu, J. (2021). Research Status of Rock Acoustic Emission. *Journal of Sichuan Normal University(Natural Science)*, *44*(05), 569-575+566.
19. Mohammadi, R., M. Saeedifar, H. H. Toudeshky, et al. (2015). Prediction of delamination growth in carbon/epoxy composites using a novel acoustic emission-based approach. *Journal of Reinloadd Plastics& Composites,*, *34*(11), 868-878.
20. Noguchi, M., S. Okumura, and S. Kawamoto. (1985). Characteristics of acoustic emissions during wood drying. *Journal of the Japan Wood Research Society*, *31*(3), 171-175.
21. Qin, G., M. Li, S. Fang, et al. (2022). Study on the dispersion characteristics of wood acoustic emission signal based on wavelet decomposition. *Wood Research*, *67*(6), 966-978.
22. Qin, G., M. Li, S. Fang, et al. (2024). Study of a grid-based regional localization method for damage sources during three-point bending tests of wood. *Construction and Building Materials*, *419*.
23. Rescalvo, F. J., M. Rodríguez, R. Bravo, et al. (2020). Acoustic emission and numerical analysis of pine beams retrofitted with FRP and poplar wood. *Materials*, *13*(2), 435-446.
24. Shao, Z. (2007). Wood Damage-Fracture and Wood Meso-Damage Elements. *scientia silvae sinicae*, *01*(04), 107-110.
25. Shao, Z. (2009). *Fracture and damage of wood and bamboo.* [Doctor, Anhui Agricultural University].
26. Shao, Z., P. Chen, C. Za, et al. (2009). Acoustic emission characteristics of damage and fracture process of wood and felicity effect. *scientia silvae sinicae*, *45*(2), 86-91.
27. Shen, K., H. Zhao, X. Ding, et al. (2015). Acoustic emission signal wavelet disjunction in wood damage fracture process. *Journal of Henan University of Science and Technology: Natural Science*, *36*(3), 33-37.
28. Vun, R. Y., C. dehoop, and F. C. Beall. (2005). Monitoring critical defects of creep rupture in oriented strandboard using acoustic emission: incorporation of EN300 standard. *Wood Science & Technology*, *39*(3), 199-214.
29. Wang, M., T. Deng, S. Fang, et al. (2021). Generation and characteristics of simulated acoustic emission source of wood. *Journal of Northeast Forestry University*, *49*(06), 96-101+118.
30. Wang, M., M. Li, T. Deng, et al. (2021). Study on lamb wave propagation characteristics of wood sheet along texture direction. *Wood Research*, *66*(1), 141-152.
31. Xu, N., M. Li, S. Fang, et al. (2023). Research on the detection of the hole in wood based on acoustic emission frequency sweeping. *Construction and Building Materials*, *400*, 132761.
32. Zhai, E., S. Fang, M. LI, et al. (2025). Research on clustering identification of acoustic emission events in the process of wood crack propagation using PCA. *Wood Research*, *69*(4), 647-660.
33. Zhang, M., Q. Zhang, J. Li, et al. (2021). Classification of acoustic emission signals in wood damage and fracture process based on empirical mode decomposition, discrete

wavelet transform methods, and selected features. *Journal of Wood Science*, *67*(1), 59.

KUN DU, XINLIN LI, SAIYING FANG, HAO SHI, YONGYOU CHEN, XUANRUI GONG
SOUTHWEST FORESTRY UNIVERSITY
BAILONG ROAD 300, PANLONG DISTRICT, KUNMING
CHINA

YOULI WANG, LIJIAN YUAN
YUNNAN VOCATIONAL INSTITUTE OF ENERGY TECHNOLOGY
WENYUAN NORTH ROAD, VOCATIONAL EDUCATION PARK, QUJING
CHINA

MING LI*
ANHUI POLYTECHNIC UNIVERSITY, BEIJING MIDDLE ROAD, WUHU, CHINA
KEY LABORATORY OF ADVANCED PERCEPTION AND INTELLIGENT CONTROL
OF HIGH-END EQUIPMENT OF MINISTRY OF EDUCATION
CHINA
*Corresponding author: 1841719811@qq.com